

This is an Open Access document downloaded from ORCA, Cardiff University's institutional repository:<https://orca.cardiff.ac.uk/id/eprint/149622/>

This is the author's version of a work that was submitted to / accepted for publication.

Citation for final published version:

Clifton, Nicholas , Bosworth, Matthew , Haan, Niels, Rees, Elliott , Holmans, Peter , Wilkinson, Lawrence , Isles, Anthony , Collins, Mark and Hall, Jeremy 2022. Developmental disruption to the cortical transcriptome and synaptosome in a model of SETD1A loss-of-function. *Human Molecular Genetics* 31 (18) , pp. 3095-3106. 10.1093/hmg/ddac105

Publishers page: <https://doi.org/10.1093/hmg/ddac105>

Please note:

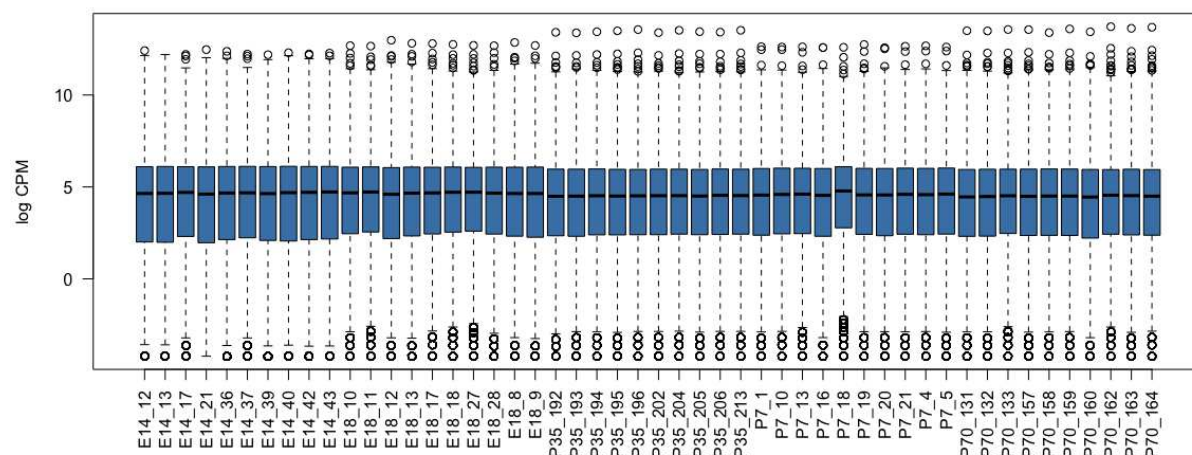
Changes made as a result of publishing processes such as copy-editing, formatting and page numbers may not be reflected in this version. For the definitive version of this publication, please refer to the published source. You are advised to consult the publisher's version if you wish to cite this paper.

This version is being made available in accordance with publisher policies. See <http://orca.cf.ac.uk/policies.html> for usage policies. Copyright and moral rights for publications made available in ORCA are retained by the copyright holders.

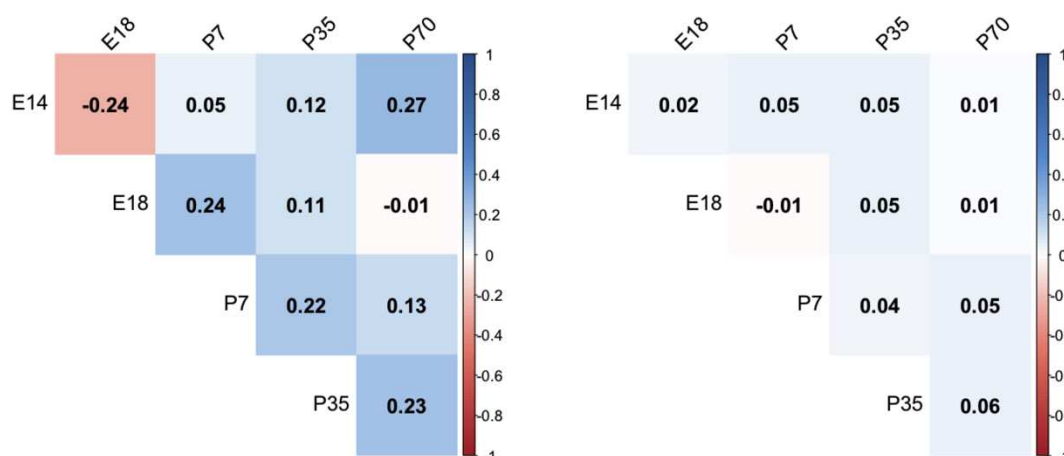


Developmental disruption to the cortical transcriptome and synaptosome in a model of *SETD1A* loss-of-function

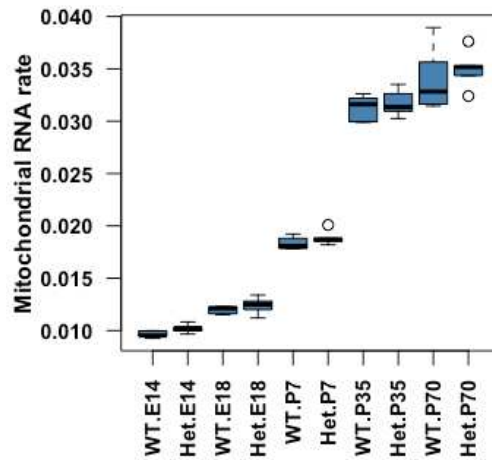
Supplementary Information



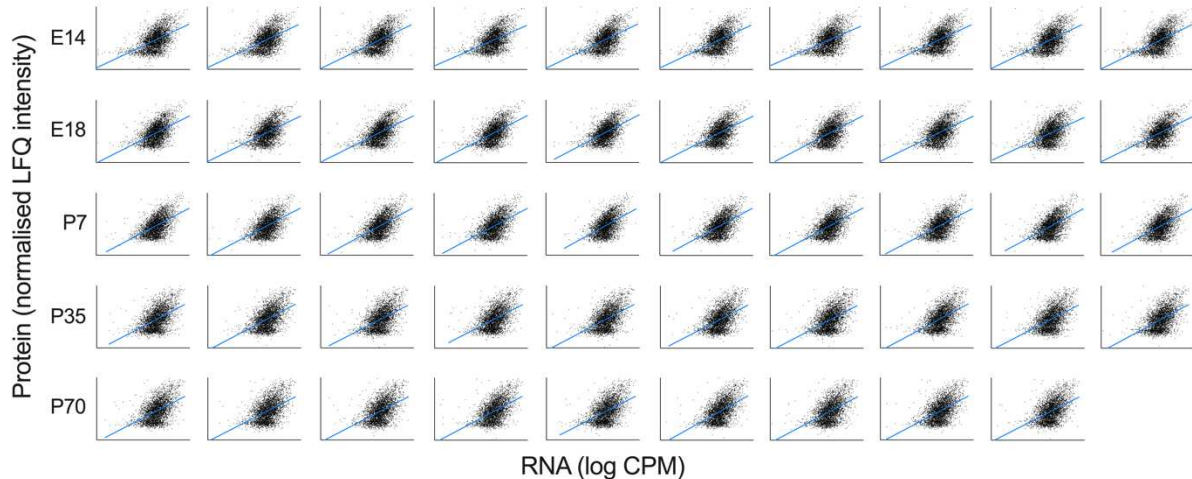
Supplementary Figure S1 Read counts distribution following RNA sequencing of 50 cortical samples from wildtype mice and mice carrying a loss-of-function mutation in *Setd1a*, across five developmental stages. Data is presented in $\log_2(\text{counts per million})$.



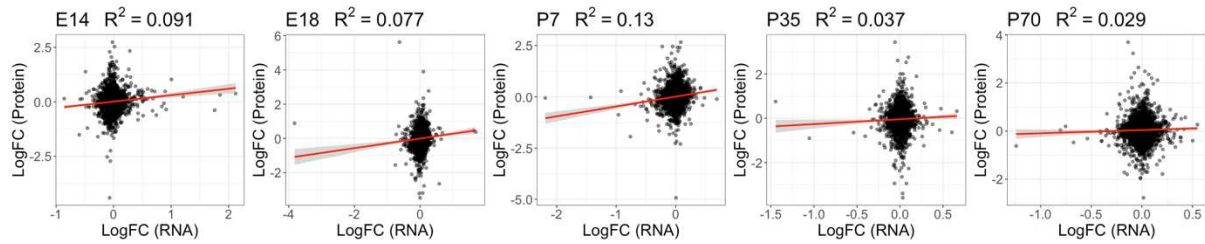
Supplementary Figure S2 Comparisons of differential gene (left) or protein (right) expression across five developmental stages. Shown are pairwise Pearson correlation coefficients between the log fold change observed for each gene or protein in genotype contrasts at each stage. Colours indicate the strength and direction of the correlation.



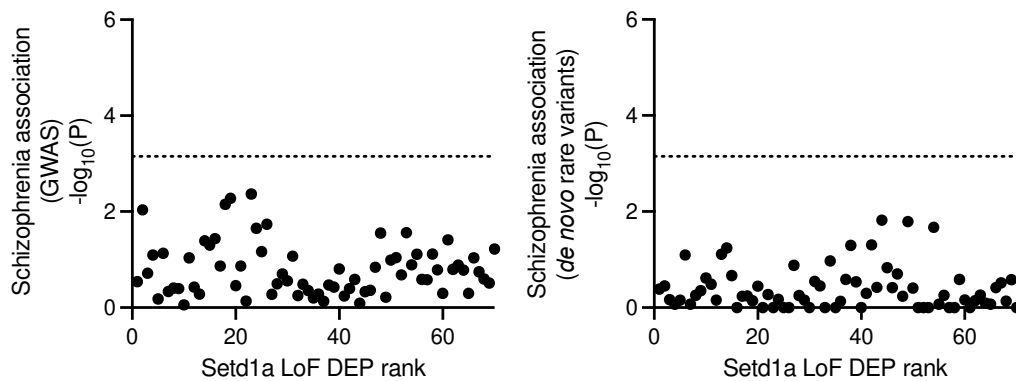
Supplementary Figure S3 Comparison of the proportion of read counts aligned to the mitochondrial genome in cortical samples from wildtype and *Setd1a*^{+/-} mice at five stages of development. Wildtype (WT); Heterozygous (Het).



Supplementary Figure S4 RNA-protein correlation of the synaptosome in 49 cortical samples. RNA sequencing of bulk tissue and mass spectrometry-based label-free quantitation of isolated synaptosomes was performed using tissue from frontal cortex of wildtype and *Setd1a*^{+/-} mice. One P70 sample processed for protein quantification was not subjected to RNAseq due to replacement during quality control. Median $R^2 = 0.24 \pm 0.017$.



Supplementary Figure S5 Comparisons of differential gene expression with differential protein expression at five developmental timepoints. Plotted are log fold changes for each synaptosomal gene and its corresponding protein following contrasts between cortical tissue from wildtype and *Setd1a*^{+/-} mice at each age. R² values correspond to the Pearson correlation coefficient.



Supplementary Figure S6 Schizophrenia genetic association of binned sets of proteins ranked by probability of differential expression in the synaptosome of frontal cortical tissue from *Setd1a*^{+/-} mice compared to wildtype controls. Each bin contains 50 genes. Shown is $-\log_{10}(P)$ -value) in one-tailed gene set enrichment analyses using common variants (left) or *de novo* rare variants (right).

Supplementary Table S1 RNA sequencing sample metadata

Sample ID	Age	Genotype	RNA Integrity	Raw reads
E14_12	E14	WT	8.1	79694358
E14_13	E14	Het	9.8	79911750
E14_17	E14	Het	9.9	84955826
E14_21	E14	WT	9.6	88454156
E14_36	E14	Het	9.5	86956670
E14_37	E14	Het	9.8	86827146
E14_39	E14	WT	10	93642210
E14_40	E14	WT	10	83172116
E14_42	E14	Het	9.9	94630422
E14_43	E14	WT	9.9	90555812
E18_10	E18	Het	9.8	83098980
E18_11	E18	WT	9.9	82988784
E18_12	E18	Het	8.1	84519088
E18_13	E18	WT	8.7	84856574
E18_17	E18	Het	6.8	79691188
E18_18	E18	WT	10	82975144
E18_27	E18	WT	9.7	84936680
E18_28	E18	Het	9.6	91058580
E18_8	E18	Het	7.8	85170458
E18_9	E18	WT	9.9	88822842
P35_192	P35	Het	8.8	96081558
P35_193	P35	WT	8.9	83699420
P35_194	P35	Het	8.9	86449832
P35_195	P35	WT	8.5	88274004
P35_196	P35	Het	8.6	82942578
P35_202	P35	WT	9	83955372
P35_204	P35	Het	8.7	81787242
P35_205	P35	Het	9.1	87622142
P35_206	P35	WT	8.9	83568088
P35_213	P35	WT	8.9	83351912
P7_1	P7	Het	9.7	82990994
P7_10	P7	Het	9.4	81501550
P7_13	P7	WT	9.6	85822912
P7_16	P7	Het	9.8	83329092
P7_18	P7	WT	9.7	85054368
P7_19	P7	Het	9.7	82828370
P7_20	P7	WT	9.6	82452790
P7_21	P7	WT	9.6	84390560
P7_4	P7	WT	9.9	82446960
P7_5	P7	Het	9.8	87511448
P70_131	P70	Het	9	83814238
P70_132	P70	WT	9	84029636
P70_133	P70	Het	8.4	83694650
P70_157	P70	Het	9.3	85776580
P70_158	P70	WT	6.7	86171434
P70_159	P70	Het	8.4	83081626
P70_160	P70	WT	8.5	84000502
P70_162	P70	WT	8.5	83499260
P70_163	P70	WT	8.7	89064386
P70_164	P70	Het	8.7	82100618